Scars in Groups of Eigenstates in a Classically Chaotic System

G. G. de Polavieja and F. Borondo
Departamento de Química, C-IX, Universidad Autónoma de Madrid, Cantoblanco 28049 Madrid, Spain

R. M. Benito
Departamento de Física Aplicada, Escuela Técnica Superior de Ingenieros de Telecomunicación, Universidad Politécnica de Madrid, 28040 Madrid, Spain
(Received 19 April 1993)

A general method to construct wave functions highly localized on a given periodic orbit, using the information contained in the short term quantum dynamics of the system, is presented. The relationship with the Husimi's quasiprobability distribution in phase space is also discussed.

PACS numbers: 05.45.+b, 03.65.Ge, 03.65.Sq

In the past few years considerable attention has been paid to study the connection between classical and quantum dynamics in situations where classical chaos dominates [1]. In a series of papers, Gutzwiller constructed a semiclassical version of the quantum mechanical Green's function in terms of classical orbits, and applied it to the calculation of eigenvalues of classically chaotic systems [2]. Berry [3] and Voros [4], based on the theorem of Schnirelman [5], formulated the conjecture that the quantum expectation value of a smooth operator is the classical microcanonical average, for almost all states. Accordingly, the high lying wave functions would be the projection of the classical microcanonical distribution on the coordinate space. The numerical studies and theoretical arguments of McDonald and Kaufman [6] and Heller [7] on the Bunimovich stadium have proved this conjecture to be incomplete, since some eigenfunctions appear strongly "scarred" by certain unstable periodic orbits (PO). This localization effect on individual eigenstates can also be studied by considering quasiprobability density distributions in phase space, such a Wigner or Husimi's distributions [8,9]. However, no general conditions or criteria have been given, so far, for the occurrence of this effect.

Using Gutzwiller's summation formulas, Bogolmony [10] obtained an expression for the smoothed quantum probability density over small intervals in energy and in space. These averaged probabilities over groups of eigenstates have, superimposed to the microcanonical distribution term, contributions localized around closed classical paths. It is worth noting that, due to the smoothing over an energy interval, contributions arising from long orbits are eliminated.

Another interesting contribution is that of Nishioka, Hansen, and Mottelson [11] that for spherical mean field potentials for electrons in metal clusters, found a relation between the oscillations of the low resolution version of the quantum density of states and classical POs and its interference.

Heller's work has also introduced a quantum dynamical viewpoint into the picture we have described above [12]. The relationship existing between spectra and wave-packet dynamics has helped to understand the localization phenomena [13] and permitted the connection with experiments [12,14]. Recently, Tomsovic and Heller have shown that some quantum eigenstates of chaotic systems can be constructed semiclassically [15].

In the spirit of Bogolmony's theory, we present in this Letter a general method to construct a sequence of nonstationary wave functions highly localized on a given PO, each one corresponding to an increasing degree of excitation in the mode represented by the PO. The new localized wave functions are obtained as linear combination of eigenfunctions of the system under consideration, where the coefficients and energy interval are determined solely from the short term quantum dynamics (wave-packet propagation) of the system. This represents a numerical way of extracting the information concerning a particular PO contained in a group of eigenstates. (Natural units, i.e., $\hbar = 1$, $m = 1$, will be used throughout.)

The results that we are presenting in this work correspond to the quartic oscillator

$$H = \frac{1}{2}\left(P_x^2 + P_y^2\right) + \frac{1}{2}x^2y^2 + \frac{\gamma}{4}(x^4 + y^4) \qquad (1)$$

with $\gamma = 0.01$. The classical motion of this system for $\gamma \to 0$ was thought for a long time to be completely chaotic, i.e., all periodic orbits to be unstable. However, Dahlquist and Russberg found the existence of a family of stable periodic orbits [16]. The Hamiltonian (1) exhibits mechanical similarity: the properties of the classical motion at any energy can be determined by scaling from $E = 1$; this avoids the complications derived from the dependence of phase space structure on the energy. A very interesting review on the quartic potential has recently appeared in the literature [17].

Several theoretical studies of system (1), which are relevant to the points addressed in this Letter, have been presented in the literature. Waterland *et al.* [9] constructed quantum surfaces of section (QSOS) by calculating the squared overlap of the eigenfunctions with a harmonic oscillator coherent state (Husimi distribution), centered at a point on the classical surface of section.

0031-9007/94/73(12)/1613(4)$06.00

They found that some states are scarred by short PO's and their QSOS affected by the corresponding stable and unstable manifolds. Eckhardt, Hose, and Pollak [18] presented a comprehensive study of the eigenfunctions of system (1) showing that many of them were scarred by PO's. They also established the importance of the adiabatic stability of the PO for the localization of some specific states, i.e., those which localize along both axis.

The quantum eigenstates of the quartic oscillator (1) can be classified according to the C_{4v} symmetry group, which has five irreducible representations: A_1, B_1, A_2, B_2, and E. The corresponding eigenvalues and eigenfunctions have been calculated using a basis set of symmetry adapted two-dimensional harmonic oscillator functions. The lowest 700 states of the A_1 symmetry class were converged to five significant figures. Similarly to the results of Eckhardt, Hose, and Pollak around half of the calculated eigenfunctions are localized around a few short PO's. The other half show a much more complicated pattern, and it has been argued that they may be the result of the interference of many PO's [19].

To gain more information on the scarring effect of the PO's on eigenstates density patterns we will follow the dynamics of a wave packet initially placed in phase space in the vicinity of a particular PO

$$\phi\left(x,y;x_0,y_0,P_x^0,P_y^0\right)=(2\alpha/\pi)^{1/4} \times\exp\left[-\alpha(x-x_0)^2-\alpha(y-y_0)^2\right] \times\exp\left[i\left(P_x^0x+P_y^0y\right)\right] \tag{2}$$

with $\alpha = 1/2$.

The dynamics of this nonstationary state can be followed—very conveniently in our case since it is a bound system—by studying the infinite resolution spectrum

$$I_\infty(E) = \frac{1}{2\pi}\int_{-\infty}^{\infty} dt\,\langle\phi(0)\,|\phi(t)\rangle e^{-iEt} = \sum_n |\langle\phi(0)\,|n\rangle|^2\delta(E-E_n), \tag{3}$$

where $|n\rangle$ is the nth eigenstate of the system.

As a working example, we chose our initial wave packet to be initially centered at $(x_0, y_0, P_x^0, P_y^0) = (2.769\,90, 0, 0, 7.050\,225)$, so that the short term dynamics is expected to closely follow that of the "box-type" PO. This orbit, shown in Fig. 1, is highly unstable (stability exponent $\kappa = 5.5842$), and has been considered in Refs. [9] and [18]. For the sake of making the presentation simpler, we only consider the spectrum obtained by using an A_1 symmetry adapted initial wave packet, thus eliminating all contributions not belonging to this symmetry class. The corresponding infinite spectrum, shown in the lower part of Fig. 1 in the form of a stick spectrum, is very complex. This result if not unexpected since it contains information on the long term dynamics of the wave packet. A way to simplify the spectrum is to consider its low resolution, finite time version

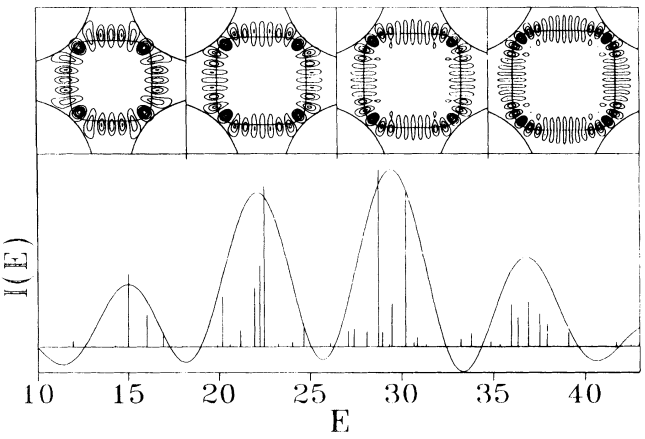

FIG. 1. Infinite resolution stick spectrum $I_\infty(E)$ and its low resolution version $I_T(E)$ (lower panel) for a wave packet initially centered on the box-type PO at an energy of 25.0. Squared band wave functions, calculated with Eq. (5), corresponding to each band are shown in upper panel; the box-type PO's and the equipotential lines at the energies of the center of the bands (see Table I) are also included.

$$I_T(E) = \frac{1}{2\pi}\int_{-T}^{T} dt\,\langle\phi(0)\,|\phi(t)\rangle e^{-iEt} \tag{4}$$

with T the recurrence time of the correlation function $\langle\phi(0)\,|\phi(t)\rangle$, around one-fourth of the classical period of the box-type PO. The result is also presented in Fig. 1, as a smooth curve, superimposed on the original stick spectrum. It is apparent that it shows a much simpler and regular pattern, consisting only of four roughly equally spaced bands.

The wave function associated to each of these bands can be calculated in a straightforward manner

$$\Psi^{\text{band}} = \frac{1}{2\pi}\int_{-\tau}^{\tau} dt\,|\phi(t)\rangle e^{iE_0t} = \sum_n |n\rangle\langle n|\phi(0)\rangle\,\frac{\sin(E_0-E_n)\tau}{\pi(E_0-E_n)\tau} \tag{5}$$

where E_0 is the energy corresponding to the center of the band and τ the time associated to its width. Approximated formulas similar to (5) have been used in Refs. [20].

The results for the band wave functions, calculated using the exact expression (5), are shown in the upper part of Fig. 1, where we have placed each function on top of the corresponding band [21]. The box-type PO's and the equipotential lines calculated at the energies of the center of each band are also included. It is clearly shown that the calculated band wave functions appear very localized in the region around the PO, with an increasing number of nodes along it.

Let us consider now in more detail the localization mechanism of the projection defined in Eq. (5). In Fig. 2, we present the four eigenfunctions contributing the most to the fourth band in $I_T(E)$ of Fig. 1 [21]. None of them show a preferred localization on the PO

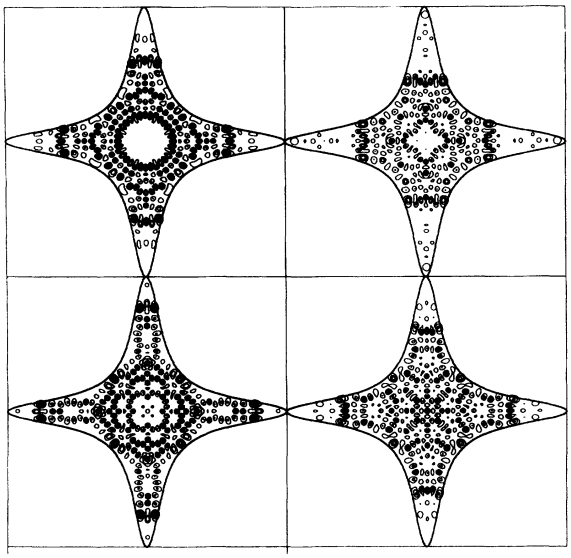

FIG. 2. The four (squared) eigenfunctions contributing the most to the fourth band wave function of Fig. 1. They correspond to the 63th, 65th, 66th, and 67th states of A_1 symmetry with energies 76.169, 76.948, 77.154, and 77.581, respectively. Remark that none of them show a preferred localization; it is the effect of the linear combination in Eq. (5) which localize the resulting band wave function on the box-type PO, as shown in Fig. 1.

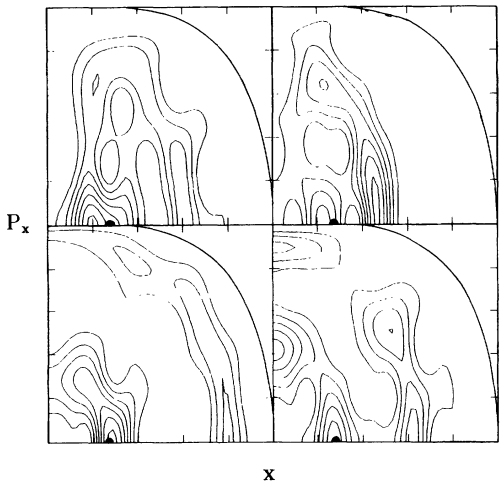

FIG. 3. Contour plots of the QSOS for the four eigenfunctions presented in Fig. 2. The boundary of the energy shell is also included. Only the first quadrant is presented. Notice that all of the QSOS have important values at the phase point corresponding to the box-type PO, which is marked by semicircles in the figure.

under consideration, and they present important density values in other regions of configuration space. However, some localization can be seen in the corresponding quasiprobability distributions in phase space, given, for example, by the QSOS defined by the cut of Husimi function corresponding to $y = 0$ and P_y given by the state eigenenergy. The results are presented in Fig. 3 [22], where it is apparent that all of them have important values at the phase points corresponding to the box-type PO (indicated by semicircles in the figure). Nevertheless, the QSOS present substantial values in other regions of the available phase space. It is the effect of the coefficients $\langle n|\phi(0)\rangle$, weighting the eigenfunctions in Eq. (5), which cancels contributions from other regions of phase space, making the appropriate linear combination of eigenstates which localize the band wave functions over the desired PO. In fact, the modulus of the coefficients $\langle n|\phi(0)\rangle$ is the value of the QSOS at the phase space points which corresponds to the box-type PO.

More insight into this localization mechanism can be obtained from a semiclassical perspective. The key point is that our results refer to short term dynamics. For short times the dynamics of the true (nonintegrable) Hamiltonian does not differ very much from that of a suitable integrable approximation to it; the initial Gaussian wave packet would remain approximately Gaussian, and in the vicinity of the box-type PO hyperbolic point analytical formulas for the short time correlation function and the corresponding convoluted spectra can be obtained. This shows clearly the connection between the localization of the wave function and the existence of peaks in the convoluted spectrum. Motions with a long recurrence time (compared to the characteristic time of the perpendicular unstable mode) will then not show this effect. Also, from a practical point of view, POs with complicated patterns will show, in general, recurrence times before the one corresponding to the PO period, distorting the convoluted spectrum, and the right coefficients in Eq. (5) cannot be obtained.

We have performed a semiclassical analysis of the low resolution version of the spectrum presented in Fig. 1. In this case, and due to the mechanical similarity, this analysis can be easily carried out from a single calculation by using the scaling relations $S/S_0 = (E/E_0)^{3/4}$ and $T/T_0 = (E/E_0)^{-1/4}$. The results can be found in Table I,

TABLE I. Semiclassical analysis of the low resolution spectra of Figs. 1 and 4. Classical action (S), frequency (ω), and Lyapunov exponent (λ) for the "box-type" PO at the energies (E) satisfying the quantization conditions $S = 4n + 1$ for $n = 3, 4, 5, 6, 15, 16, 17, 18, 19, 20$. The values of E and 2λ should be compared to the position (E_{band}) and width (Γ) of the low resolution bands, whose values, obtained from Figs. 1 and 4, are given in the last two columns.

E	S	ω	$2\lambda = \kappa\omega/\pi$	E_{band}	Γ
15.4989	13.0000	1.589 63	2.8256	14.96	2.90
22.1637	17.0000	1.738 33	3.0900	22.06	3.58
29.3766	21.0000	1.865 18	3.3154	29.33	3.62
37.0649	25.0000	1.976 80	3.5138	36.83	3.22
121.745	61.0000	2.660 99	4.7299	121.6	4.36
132.514	65.0000	2.718 16	4.8315	132.6	5.34
143.497	69.0000	2.772 90	4.9288	143.1	6.54
154.694	73.0000	2.825 03	5.0215	153.9	5.28
166.098	77.0000	2.876 16	5.1124	165.1	5.04
177.701	81.0000	2.917 73	5.1863	176.2	6.24

where we are presenting the classical action, the frequency, and the Lyapunov exponent calculated at the energies satisfying the quantization condition $S = 4n + 1$ for $n = 3, 4, 5, 6, 15, 16, 17, 18, 19$, and 20, n being the number of nodal lines in the fundamental domain of the A_1 band wave functions. These actions correspond to band wave functions of A_1 symmetry, due to the form that we have chosen for the initial wave packet. By appropriately choosing the symmetry of the initial wave packet, the band wave functions of other symmetries, associated to intermediate actions, could be obtained. Alternatively, a spectrum containing all symmetries can be obtained from a single calculation by using an initial wave packet without any symmetry, for example, a single coherent state centered in the vicinity of the PO. For the sake of comparison with the low resolution spectrum of Fig. 1, we have included in the last two columns the energies at the center of the bands and their widths. The position of the bands, its separation, and their widths should correspond respectively to the quantized energies, 4 times (due to the A_1 symmetry chosen for the initial wave packet) the frequency, and 2 times [23] the Lyapunov exponent of the box-type PO [7]. As can be seen in Table I the agreement is quite good. Thus, the PO quantization seems to account completely for the bands energies, and no zero-point energy contribution from the perpendicular motion to the PO appears.

Finally, we address the question of how powerful our method is. For that purpose, we have calculated more spectra at higher energies. In Fig. 4 we present the spectrum corresponding to a wave packet initially centered at $(x_0, y_0, P_x^0, P_y^0) = (4.335\,128, 0, 0, 17.269\,45)$ corresponding to the phase space point of the box-type PO at an energy of 150.0. Clearly the band structure is robust and survives at this high energy (or equivalently at small $\hbar$), although many more states contribute significantly to each band. Results concerning the band wave functions for this spectrum and for other PO will be presented elsewhere.

To conclude, we have presented a method to reveal the information concerning a PO contained in a group of eigenstates in a chaotic Hamiltonian system. The results are particularly striking in those cases, such as those presented here, in which several eigenstates are involved.

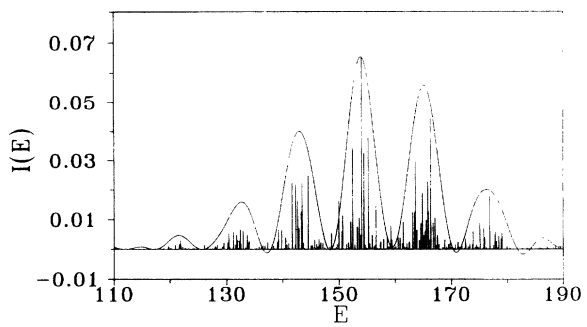

FIG. 4. Same as lower panel of Fig. 1 for a wave packet initially centered on the box-type PO at energy 150.0.

On the other hand, in situations where only one, or a few, states are relevant, the scars due to the PO are easily discernible.

This work has been supported in part by DGICYT (Spain) under Project PB92-181.

[1] M.C. Gutzwiller, *Chaos in Classical and Quantum Mechanics* (Springer-Verlag, New York, 1990); K. Nakamura, *Quantum Chaos: A New Paradigm of Nonlinear Dynamics* (Cambridge Univ. Press, Cambridge, 1993).
[2] M.C. Gutzwiller, J. Math. Phys. **12**, 343 (1971); Phys. Rev. Lett. **45**, 150 (1980).
[3] M.V. Berry, J. Phys. A **10**, 2083 (1977).
[4] A. Voros, in *Stochastic Behaviour in Classical and Quantum Hamiltonian Systems*, edited by G. Casati and J. Ford (Springer-Verlag, Berlin, 1979).
[5] A.I. Shnirelman, Ups. Mat. Nauk. **29**, 181 (1974). See also the results of S. Zelditch, Duke Math. J. **55**, 919 (1987); Y. Colin de Verdiere, Commun. Math. Phys. **102**, 497 (1985).
[6] S.W. McDonald and A.N. Kaufman, Phys. Rev. Lett. **42**, 1189 (1979); Phys. Rev. A **37**, 3067 (1988).
[7] E.J. Heller, Phys. Rev. Lett. **53**, 1515 (1984); E.J. Heller, in *Chaos and Quantum Physics*, edited by M.J. Giannoni, A. Voros, and J. Zinn-Justin (Elsevier, Amsterdam, 1991).
[8] M. Hillery, R.F. O'Connell, M.O. Scully, and E.P. Wigner, Phys. Rep. **3**, 121 (1984).
[9] R.L. Waterland, J.M. Yuan, C.C. Martens, R.E. Gillilan, and W.P. Reinhardt, Phys. Rev. Lett. **61**, 2733 (1988).
[10] E.B. Bogolmony, Physica (Amsterdam) **31D**, 169 (1988).
[11] N. Nishioka, K. Hansen, and B.R. Mottelson, Phys. Rev. B **42**, 9377 (1990).
[12] E.J. Heller, Acc. Chem. Res. **14**, 368 (1981).
[13] See for example, P.W. O'Connor and E.J. Heller, Phys. Rev. Lett. **61**, 2288 (1988).
[14] E.J. Heller, J. Chem. Phys. **68**, 3891 (1978); K. Kulander and E.J. Heller, J. Chem. Phys. **69**, 2439 (1978).
[15] S. Tomsovic and E.J. Heller, Phys. Rev. Lett. **70**, 1405 (1993); Phys. Rev. E **47**, 282 (1993).
[16] P. Dahlquist, and G. Russberg, Phys. Rev. Lett. **65**, 2837 (1990).
[17] O. Bohigas, S. Tomsovic, and D. Ullmo, Phys. Rep. **2**, 43 (1993).
[18] B. Eckhardt, G. Hose, and E. Pollak, Phys. Rev. A **39**, 3776 (1989).
[19] D. Wintgen and A. Hönig, Phys. Rev. Lett. **63**, 1467 (1989).
[20] J.M. Gomez-Llorente, F. Borondo, N. Berenguer, and R.M. Benito, Chem. Phys. Lett. **192**, 430 (1992).
[21] Note that the scale of the wave functions plots can be easily obtained from the equipotentials since, for example, $x_{\max} = y_{\max} = \pm(4E/\gamma)^{1/4}$.
[22] The scale for the QSOS plots in Fig. 3 can be easily obtained from the boundaries of the energy shell, i.e., $x_{\max} = (4E/\gamma)^{1/4}$ and $p_{x,\max} = (2E)^{1/2}$.
[23] B. Eckhardt, J.M. Gomez-Llorente, and E. Pollak, Chem. Phys. Lett. **174**, 325 (1990).